

A Topological Analysis of Art Movements

Ryan Kobler

May 3, 2023

Abstract

This study applies wavelet analysis and computes color moments in HSV space to construct a dataset of patch-level features from ten Cubist and ten Renaissance artworks to then compare the topological invariants of each art movement. Topological data analysis began by constructing a Vietoris-Rips complex filtration to identify persistent homologies in each artwork. The results illustrated that Cubism was more idiosyncratic and less cohesive than Renaissance artworks. Cubist paintings were not grouped together, reflecting the movement's emphasis on individuality and experimentation. Renaissance works, on the other hand, tended to be more grouped together, reflecting the movement's emphasis on technical skill and classical ideals. This study demonstrates the potential of topological analysis to uncover underlying patterns and structure in art history, shedding light on the nature of these two significant, often opposing, art movements.

1 Introduction

Artistic movements throughout history have been characterized by distinct styles and techniques, resulting in a rich and diverse collection of artwork. Recently, literature analyzing these movements through a mathematical lens has been growing, with applications from untangling entropy distinctions between Eastern and Western art [9] to an information theory network analysis of composition differences between landscape and portrait painting over time [6]. With the evolution of digital databases and computer vision methods, it has become feasible to extract features and conduct statistical analyses. This study takes a handful of these techniques and includes topological data analysis (TDA) methods to study differences between art movements, specifically between Cubism and Renaissance. To do so, visual features in candidate works of art from each movement were extracted by splitting each image into a set of overlapping patches and investigating color information and textures with wavelet decomposition within each. From these features I construct patch-level data to then extract topological invariants at multiple levels of analysis: between the two movements, between paintings, and within paintings.

2 Data

All data for this study come from [Google's Arts & Culture](#) application, which groups artworks by several categories, including by art movement. Google identifies at least 121 art movements, 6,272 total artists, and features content from over 2000 leading museums and archives who have partnered with the Google Cultural Institute. For this study, I focus on 10 Cubist and 10 Renaissance artworks and with increased computing resources, this analysis could easily be extended to include more artworks per movement and additional movements. However, the focus is upon the two because they represent two vastly different movements not only in time but also visually, and recognizably, in texture and color. The selection of the pieces was from a range of popular works that I chose and thus is not a random selection from the database.

2.1 Renaissance Artworks

Renaissance was an art movement consisting of art produced during the 14th through 16th centuries in Europe characterized by increased awareness of nature, revival of classical antiquity concepts and a more individualistic view of mankind. Renaissance interest in humanism contributed to some of the most realistic representations of the human figure, using tools of contrapposto to define figures stance and increase the sense of accurate anatomy. Figures also appear to occupy plausible space, a feat attributed to development of linear and atmospheric perspective artistic techniques [2]. This focus upon realism was in part driven by the growing popularity of oil paint, a more flexible medium and new artistic techniques. Chiaroscuro (strong contrast between light and dark to create depth), sfumato (subtle blending of colors and blurring of sharp lines), and foreshortening, perspective and proportion (mathematical principals to create the illusion of depth) were all established during the Renaissance and contributed to a unified aesthetic that strove toward realism and idealism [5]. Figures [22](#) and [19](#) show the 10 Renaissance works included.

2.2 Cubist Artworks

Cubism was an art movement consisting of works largely between 1907-1921 and came from a term derived from a reference made to “geometric schemas and cubes”, (a subtle nod to geometry/topology itself) and is generally applied to work of this period by Pablo Picasso and a range of works produced in France [8]. Artists rejected the concept that art should emulate nature and that artists should paint using traditional techniques of perspective and foreshortening, instead favoring emphasis of the two-dimensionality of the canvas and fracturing objects into geometric forms. These fractured forms would then be realigned via multiple perspective points. In this way, Cubist painters rebuffed many of the techniques couched in realism Renaissance painters established and honed. Figures [16](#) and [17](#) show the 10 works included in this study.

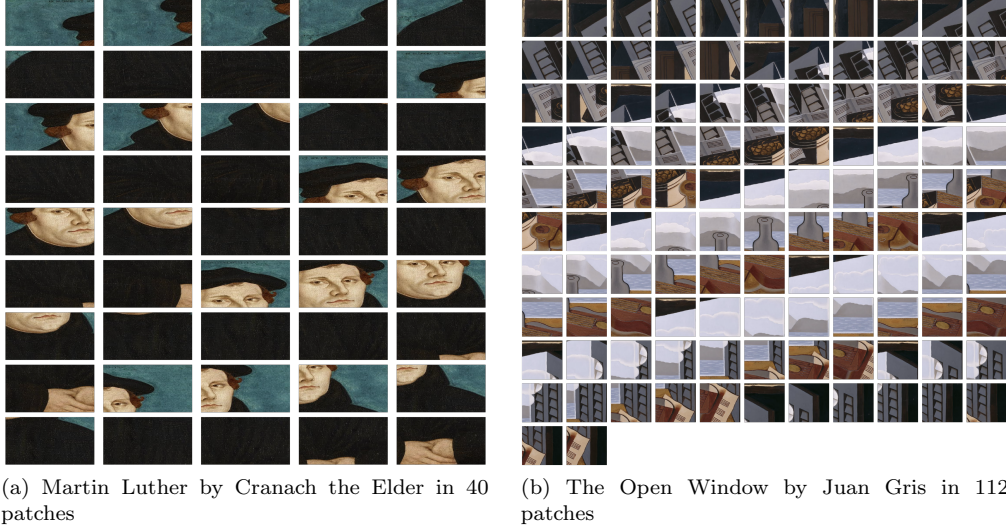


Figure 1: Image patches each of size 256 x 256 pixels

3 Feature Extraction

Because the images are large with many pixels, conducting the analysis pixel by pixel was infeasible. One option was to decrease the number of pixels in each image by decreasing the resolution. However, in both these movements each image contains rich textural information which likely varies between the two. For instance in The Ambassadors, Figure 19 (d), we have complex textures depicted in the fur of the left figure's coat, the silk of his sleeves, the velvet texture and floral patterning of the curtains. Hence I divide each image into overlapping square patches of side length 256 pixels illustrated for one Renaissance and one Cubist piece in Figure 1. Dividing the original image into patches also limits the size of data processed at once making the analysis computationally cheaper.

For each patch the following attributes are extracted:

3.1 Wavelet Transform

To measure encoded textural information, each patch is processed through a multi-level wavelet decomposition, a technique that involves decomposing an image signal into a set of wavelets.

The process begins by applying a series of filters hierarchically to the (greyscale) image. A low-pass filter is first applied to the image, which preserves the low-frequency components of the image and removes the high-frequency components. This results in a set of subbands (or different approximations of the image), each containing a portion of the image but at a lower resolution. We get 4 resulting subbands for the filter applied across the image vertically (LH), horizontally (HL), diagonally (HH), and a residual subband that contains the remaining low-frequency information (LL). Next, a high-pass filter is applied to the original image which does the reverse, also resulting in 4 subbands [9].

Then, the high and low pass filter coefficients from each subband are combined to create the 4 subbands with the LL containing the most low-frequency information, HL and LH containing a

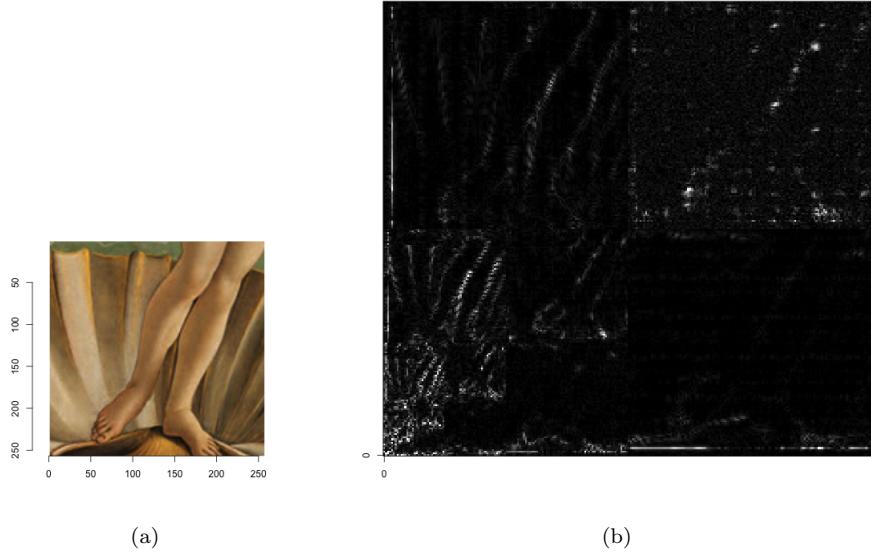


Figure 2: (a) Original Birth of Venus patch and (b) Wavelet coefficients of Birth of Venus patch. The top right contains the highest resolution diagonal coefficients, bottom right contains the horizontal coefficients, top left contains vertical coefficients, and bottom left contains the same information for the transform of the approximation image, iteratively

combination of horizontal and vertical high-frequency components. Finally, the low-pass and high-pass filters are iteratively applied to each resulting approximation image to build many layers of the four subbands at different scales [3].

To see this, consider Figure 2. Side (a) shows a patch from Birth of Venus then passed through a wavelet transform whose coefficients within the four different subbands are plotted in (b). We can see that the high frequency top right corner corresponds to the diagonal pass and contains finer textures (possibly the graininess of the image), whereas the top left detects the edge details in the vertical direction, e.g., the highlight on the right side of Venus's legs. The bottom right comprises the horizontal components, which appear to highlight Venus's feet and the bottom of the shell.

3.1.1 Textural Measures

The textural measures: energy, contrast, and energy are thus are computed from wavelet transform coefficients. The wavelet energy of a subband is the sum of squares of the wavelet coefficients:

$$E_{i,j} = \sum_k |C_{i,j,k}|^2 \quad (1)$$

where $C_{i,j,k}$ is the k th wavelet coefficient in the i th layer of decomposition and j is the subband ($j = \{HH, HL, LH, LL\}$). Hence the total energy of the image is simply the sum of the wavelet

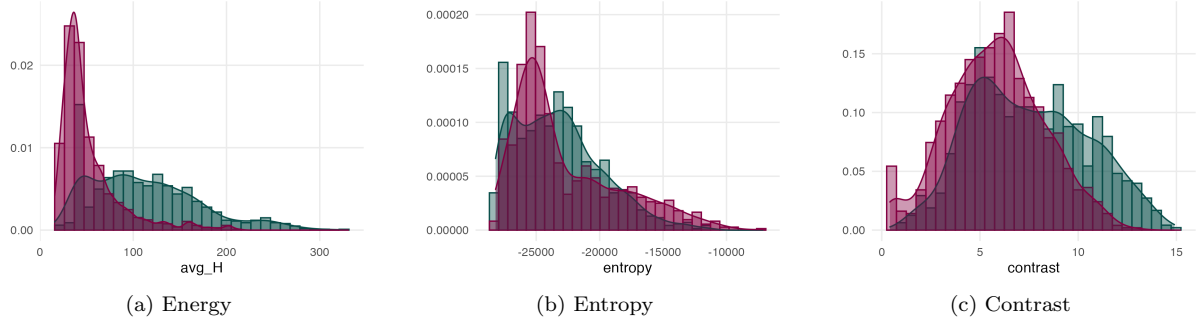


Figure 3: Overlaid density plots of textural features of patch-level data by movement, magenta is Renaissance and green is Cubism

coefficients in each subband, or

$$E_{image} = \sum_i E_i = \sum_i \sum_j E_{i,j}. \quad (2)$$

From the total energy of the image, and each individual subband's level of energy we can calculate the entropy with

$$E_t = - \sum_{i,j} \frac{E_{i,j}}{E_{image}} \cdot \log \frac{E_{i,j}}{E_{image}}. \quad (3)$$

Entropy measures the amount of uncertainty in the distribution of subband energy values in the image. Images with higher entropy, more diversity between subbands, tend to be more complex while those with low entropy have less variation over subbands and are simpler.

Finally, contrast measures the average value contrast between all subbands and layers and is computed as follows:

$$C_o = \frac{1}{N} \sum_i \max(\{C_{i,j}\}) - \min(\{C_{i,j}\}) \quad (4)$$

where N is the total number of subbands throughout all layers, i.e., $N = 4L$, where L is the number of layers.

Returning to the data, and computing these textural measures across all patches, Figure 3 illustrates these textural distributions between Renaissance and Cubism.

Overall, Renaissance is right skewed in entropy and energy while Cubism takes larger values of all three measures more often. Renaissance also tends to have more mass at the mode, indicating within movement Renaissance paintings are similar to one another in texture, while Cubism has more variance. But the two distributions overlap, so while the textural measures are informative, they don't immediately class works into movements.

Zooming in to the image level reveals variation within paintings. For example, returning to The Birth of Venus, Figure 4 shows the values of energy, entropy, and contrast with each textural feature

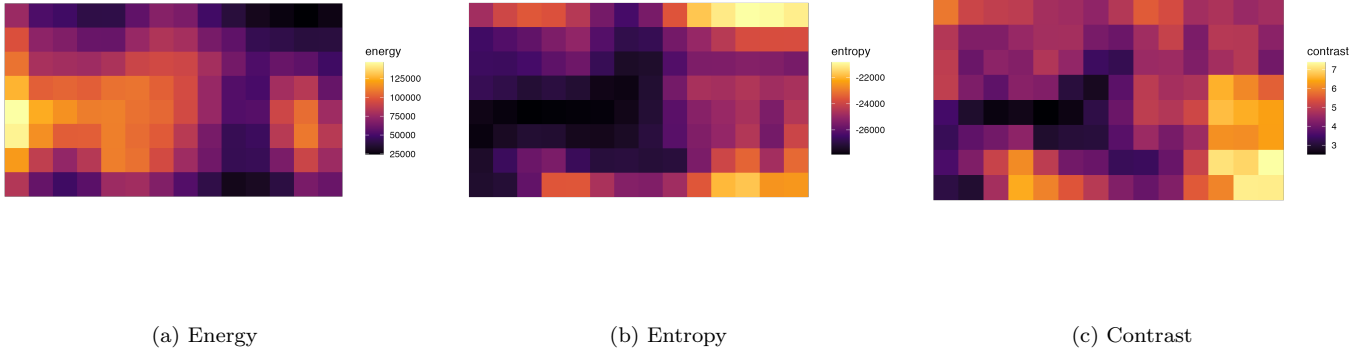


Figure 4: Patch level tile plots containing textural features in Birth of Venus painting



Figure 5: HSV Scale, top row shows changes in hue, second row changes in saturation, final row changes in value [1]

plotted in color. Energy appears largest in the brighter regions of the image - the rightmost figure’s white dress, the shimmer of the sea and sky on the left hand side. The entropy plot picks up the finer textural details of the leaves in the trees, the feathers of the wings, the speckling of the ground in the bottom right corner, the edges of the shell and waves at the bottom. In the contrast plot, the highest values are in the bottom right corner denoting the contrast between the near-black ground and the white dress. The contrast between the shadow of the shell and the shell appears in the bottom left.

To compute all textural features from the wavelet decomposition I rely on the ‘wavethresh’ package [4].

3.2 Color Space

Given that wavelet analysis operates on greyscale images, color information is lost. So color moments are computed to capture the color distribution of the image on the transformed RGB (red, green, blue) to HSV color space (hue, saturation, value). HSV is often preferred over RGB for image classification because it is more perceptually uniform. In HSV, as shown in Figure 5 the hue represents the purity of the color, the saturation channel the purity, the value channel the brightness. This separation of elements can make it easier to distinguish different colors and combinations, and is robust to changes in lighting conditions and shadows.

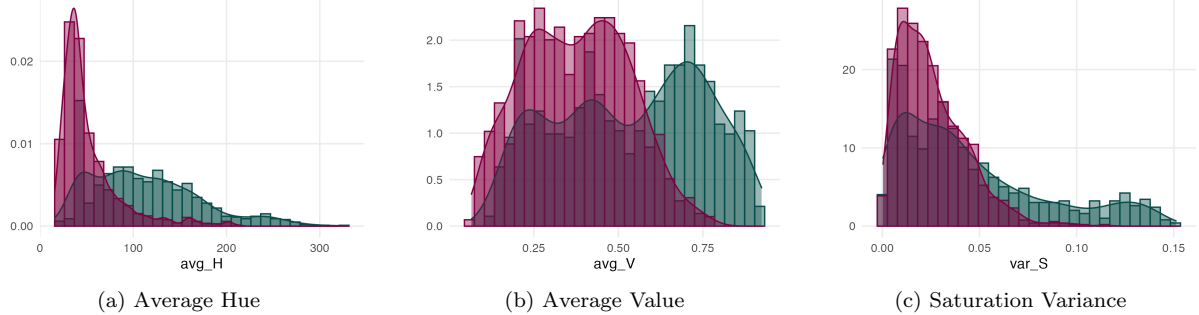


Figure 6: Overlaid density plots of color features of patch-level data by movement, magenta is Renaissance and green is Cubism

The first and second color moments are computed for each channel as follows:

$$E(C) = \sum_{i=1}^n C_i \quad (5)$$

$$\text{Var}(C) = E(C^2) - E(C)^2 \quad (6)$$

where $C \in \{H, S, V\}$ is a color channel $m \times m$ matrix of pixels within an image patch flattened to a length $2m = n$ vector and C_i is the i th coordinate of the color channel C . This gives a set of 6 features, a color average and a color variance for each channel.

Again, comparing movements and looking at the distributions of three color moments we have in Figure 6 that the average hue in Renaissance is highly right skewed. The support of the H channel is an angle value ranging from 0 to 360 degrees, in which the colors move clockwise starting from 0 as red, then yellow, cyan, blue, magenta, and back to red. Average saturation varies from 0 to 100 where 0% represents a shade of gray (fully desaturated) and 100% represents the most vivid color. Value also ranges from 0 to 100% where 0 is black and 100% is the brightest color.

From panel (a), Renaissance artwork tends to concentrate within red hues whereas Cubism varies across the color spectrum. From panel (b) we can see that Cubism paintings tend to be brighter than Renaissance and from (c) that Cubism tends to have more variance in saturation levels, but both are right skewed with low variance. Overall, the distributions of Cubism features tend to have a larger spread, suggesting a variety and diversity unmatched in Renaissance.

Zooming in on the color space of The Open Window, Figure 7 shows that the average hue of the painting aligns with the color distribution over the image, with the blues of the sky and shutters shown together in the middle and the red-brown of the table and instrument in the bottom strip indicating an average hue closer to red. Average saturation in panel (b) reveals that the colors toward the bottom of the painting in the table are more saturated than the rest of the image. We can see that the average value is high near the upper right and left corners of the window. The variances are more interesting. There we can see more hue variation toward the left hand side of the window as the table meets the window in which there are blue, brown, black white, and red-brown elements. The saturation variance

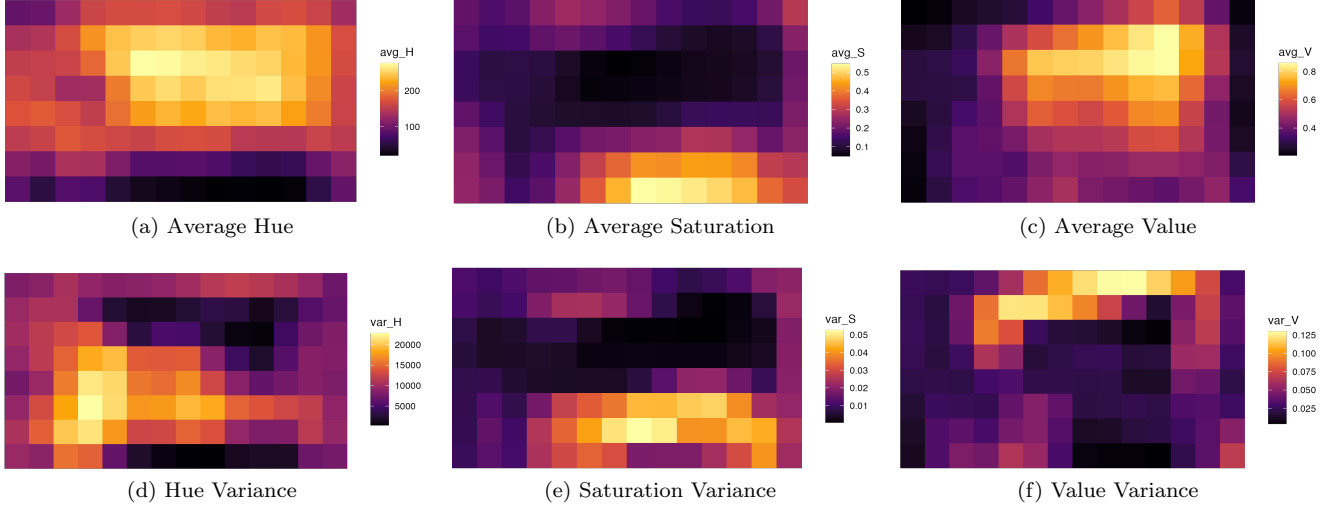


Figure 7: Patch level tile plots containing color features in The Open Window painting

highlights the table and instrument as well while omitting the entire top half of the painting. In contrast, the value variance seems to detect the window and table edges, where there is more variance between the dark part above the window and the light from the forefront window and table figures.

4 Topological Methods

The main topological methods used throughout are first constructing a distance metric to connect the generated 11-dimensional vertices to then build a continuous shape over which to compute topological invariants.

4.1 Distance Metric

The distance metric in this study is the scaled sum of the individual features, resulting in a linear combination of the Euclidean metric (also a metric). That is, we scale the 9 above texture and color features as well as the (x, y) positional coordinates of the image patch centers. Thus patches closer in position, color, and texture are more related within an image with their distances a scaled Euclidean function as written below:

$$d(\mathbf{x}, \mathbf{y}) = \sqrt{\sum_{i=1}^{11} (x_i - y_i)^2} \quad (7)$$

where \mathbf{x} corresponds to an 11 dimensional image patch with

$$\begin{aligned} \mathbf{x} &= (x_1, \dots, x_{11}) \\ &= (E(H), \text{Var}(H), E(H), \text{Var}(H), E(H), \text{Var}(H), C_o, E_t, E_{image}, X, Y). \end{aligned}$$

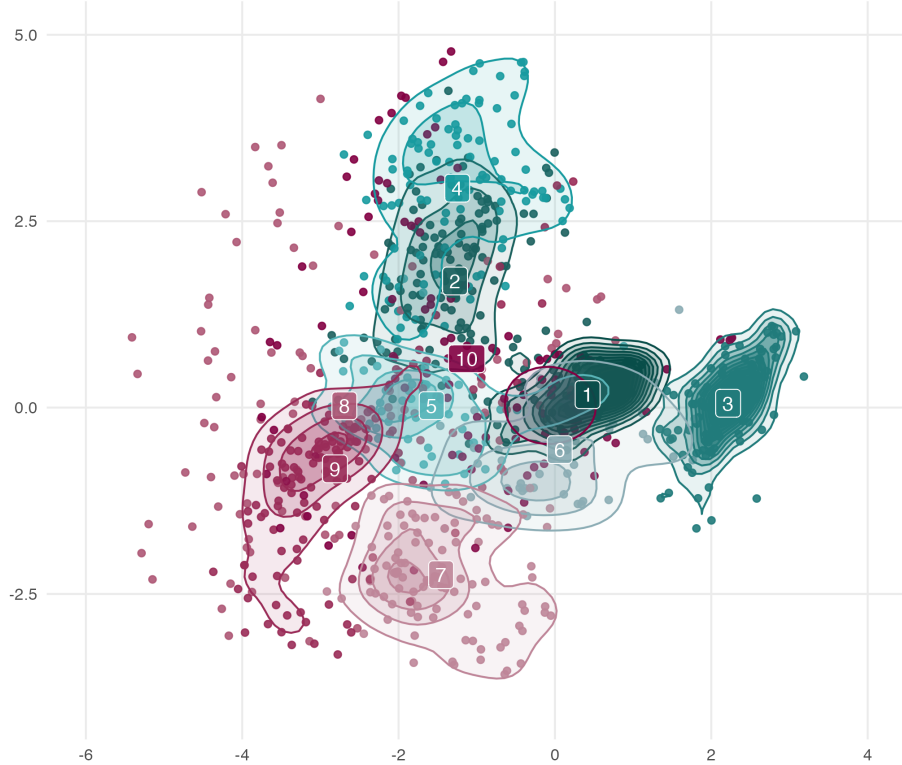


Figure 8: Scatterplot with overlaid densities colored by Cubism painting of patch-level data projected onto axes of the first two principal components

Each $x_i = \frac{\tilde{x}_i - \bar{x}_i}{s_i}$ where \tilde{x}_i is the raw unscaled i th feature of image patch vector x , and \bar{x}_i is the sample mean of the i th feature over all image patches $\{x\}_{\alpha}$. Also, $s_i = \sqrt{\frac{\sum_{i=1}^n (\tilde{x}_{ij} - \bar{x}_i)^2}{n-1}}$. The resulting data for each painting contains n rows. Because the patches are fixed in size, the number of patches per image varies. For instance, the Abstract Landscape contains 40 patches while the Portrait is larger and contains 110 patches, a potential shortcoming of the data.

For an initial glimpse into the distance between paintings, scatterplots show the relationships between any two features by movement. I aggregate all paintings from both movements and project the 11-dimensional vector into two-dimensional space via Principal Component Analysis (PCA). In essence, PCA identifies patterns and correlations among variables and transforms the data into a set of new uncorrelated, orthogonal variables referred to as the principal components. It finds linear combinations of the original variables that detect the most variance, with each subsequent principal component capturing as much of the remaining variance as possible. Here, I use the first two principal components as a basis to visualize image patches as points. Figures 8 and 9 show the space of patches projected into a basis of the first two principal components.

We can see that in Figure 8, the patches within a painting are clustered together. Specifically, painting 1 and 3 correspond to Abstract Landscape and Dinamica del Viento that are relatively uniform in texture, color, and shape throughout the painting. Comparatively, in cluster 7 (Popular Song and Bird from Brazil), color and texture vary spatially over the image resulting in a diffuse cluster. In

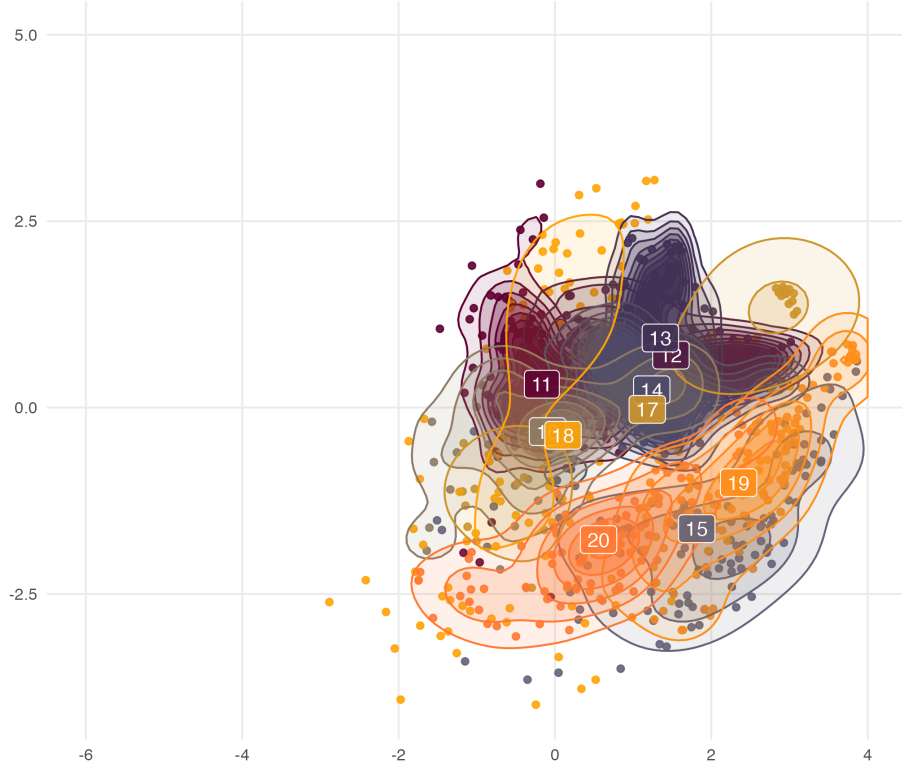


Figure 9: Scatterplot with overlaid densities colored by Renaissance painting of patch-level data projected onto axes of the first two principal components

the Renaissance version, Figure 9, all paintings glom together in a denser figure than that of Cubism. Within each painting we have more diversity of features, but between paintings these features tend to be repeated or similar to patches in other Renaissance works. That is, given a random Renaissance patch, it is more difficult to correctly identify which painting it is a part of. Notice also that the PCA scatter plots are depicted on the same axes with Renaissance paintings shifted more to the right than the Cubism group. Renaissance works are more densely clustered between -2 and 4 along the first principal component and -2.5 and 2.5 on the second principal component while Cubism works vary between -4 and 2.5 on the first component and between -2.5 and 5 on the second component. This is unsurprising given the basic distributions of Figures 3 and 6 where Cubist paintings have more spread across all features except entropy. Also, because they are plotted on the same axes, we can discern paintings that are on the cusp between Renaissance and Cubism. For example *Dinamica del Viento* is near to the Renaissance cluster in terms of the x-axis. It almost appears to split away from the rest of the Cubism point cloud. This may be because the colors are darker and hue more concentrated in black, green and yellow and hence more alike in colorspace to Renaissance works than to other Cubist works.

4.2 Vietoris-Rips Filtration

The primary mode of topological analysis in this study is via performing filtrations and tracking topological invariants. Topological invariants are non-trivial over continuous shapes, however, our patch-level data is a discrete, finite 11-dimensional point cloud. Filtration poses a solution to problem as it transforms a point cloud into continuous shapes by constructing a series of simplicial complexes (the simplest geometric objects: points, line segments, triangles, and tetrahedra) over the data. The idea boils down to recording pairwise distances between points in a series of steps. That is, for a single step of the filtration, we connect pairs of points within some distance, say ϵ_i , of one another with n dimensional edges. Then stepping through a set of increasing distance thresholds, $\{\epsilon_i\}$, gradually adds simplices to the complex over the data. This gives different versions of connected shapes over the point cloud across various levels of connectivity.

Though there are many methods to geometrically realize filtrations across various distance thresholds, for this study I use the Vietoris-Rips complex method. This simplicial complex is built by adding simplices of increasing dimension to the complex across a given $\{\epsilon_i\}$. For each ϵ_i , simplices are added to the complex until the entire point cloud is connected. The crucial Vietoris distinction is if three points $\{A, B, C\}$ are connected by edges $\{AB, BC, CA\}$, Vietoris-Rips would also fill in their face ($n + 1$ dimensional edge) $\{ABC\}$. This means connections between 1-dimensional edges, i.e, the skeleton complex, fully characterize each simplicial complex i , $\forall i$.

In this way, the Vietoris-Rips complex filtration is useful for analyzing the shape of this high-dimensional data as it lays the groundwork to visualize the underlying shape of the data in fewer dimensions with skeleton complexes, decreasing the computational cost. The resulting topological invariants (homologies)—loops, voids, and higher dimensional cavities—can be quantified using persistent homology. This technique tracks the birth and death of homologies over the Vietoris-Rips filtration as i varies and records these times in persistence diagrams where birth and death times comprise the axes.

Thresholds $\{e_i\}_j$ for painting j are selected by computing pairwise distances $\{d_i\}$ between all vertices and ordering them such that $d_i < d_{i+1}$ for all i . To ensure computational feasibility, I use d_i up to the mean distance, \bar{d} . That is, $\{d_i : d_i \leq \bar{d}\}_j$ and hence the simplicial complexes I build in the filtration are never fully connected. I focus mainly upon the H_0 homology, or connected components for the sake of interpretability (though all homologies computed are shown).

5 Results

With this potential for different scales the data was analyzed at the painting level and at the movement level.

5.1 Artwork-level

At the painting level; I performed a topological filtration for each of the 20 paintings, resulting in filtrations over a range of 40-110 observations each depending on the size of the original image. Figure 10 shows the persistence diagrams for 4 different paintings, where (a)-(c) are portraits. Here the x-axis is the birth time and y is the death time, and the points are topological features. So the higher the point above the $x = y$ 45 degree line, the more persistent that topological feature.

From these diagrams we can see that between the two Renaissance portraits (a) and (b), the H_0 homologies in purple are similar, except there is slightly more persistence in topological features just below 2 on the death axis in Martin Luther than in Jane Seymour. However, both appear to have a similar small gap midway between 2 and 3 which perhaps corresponds to components of the head of the portrait and the clothing (see Figure 11). In H_1 a similar very persistent cycle emerges between times 2 and 3 and with death time between 3.5 and 4, nonexistent in the Cubist images below.

We can also see that the Cubist Portrait in (c) has a similar, but smaller gap at the top of the H_0 cluster of points, again potentially indicating separate connected components within the woman depicted. Panel (d), which is not a portrait, doesn't contain as much separation in the number of connected components and contains more H_2 holes, albeit transient ones. There are more persistent H_1 homologies in Cubism compared with Renaissance, however another explanation could be that these Cubism pieces are slightly larger with more patches than the Renaissance portraits.

Focusing on the H_0 homologies, there is evidence from the portrait paintings that they etch out connected figures within the painting. Taking Martin Luther as an example, we can see at various distance thresholds in Figure 11, the skeleton complexes appear to represent three connected components of Martin Luther's clothing, hands, face, and the portrait background.

In panel (a) one of the first connected components is his dark coat which is similar across texture and color throughout the bottom half of image patches. However, his hands appear separate from the dark robes, depicted by the few lines and low connectivity in the bottom right. We can also see in panels (a) and (b) that initially the blue background patches were connected first, then the face, shown in the square in the upper right of (b). In (c)-(d) we have $H_0 = 1$, only one connected component, yet the skeletons of (c) and (d) convey different levels of connectivity. Connected components may not tell the entire story and visual inspection of the resulting simplicial complexes can shed additional intuition and light on persistent features. By panel (d) we lose distinction between the face and background even visually as the vertices inch closer to full connectivity. The Jane Seymour portrait follows a similar pattern with her face, clothes, and background tending to comprise distinct connected components in the early steps of the filtration.

However for the Cubism Portrait, a different pattern emerges. Parts of her clothes tend to be more connected than others—for instance the pink of her sleeves and purple near her legs are separate. Simplices are drawn in the middle of the artwork, near her arms, hands, and her instrument such that the background integrates more with the figure. This may be because the background is more

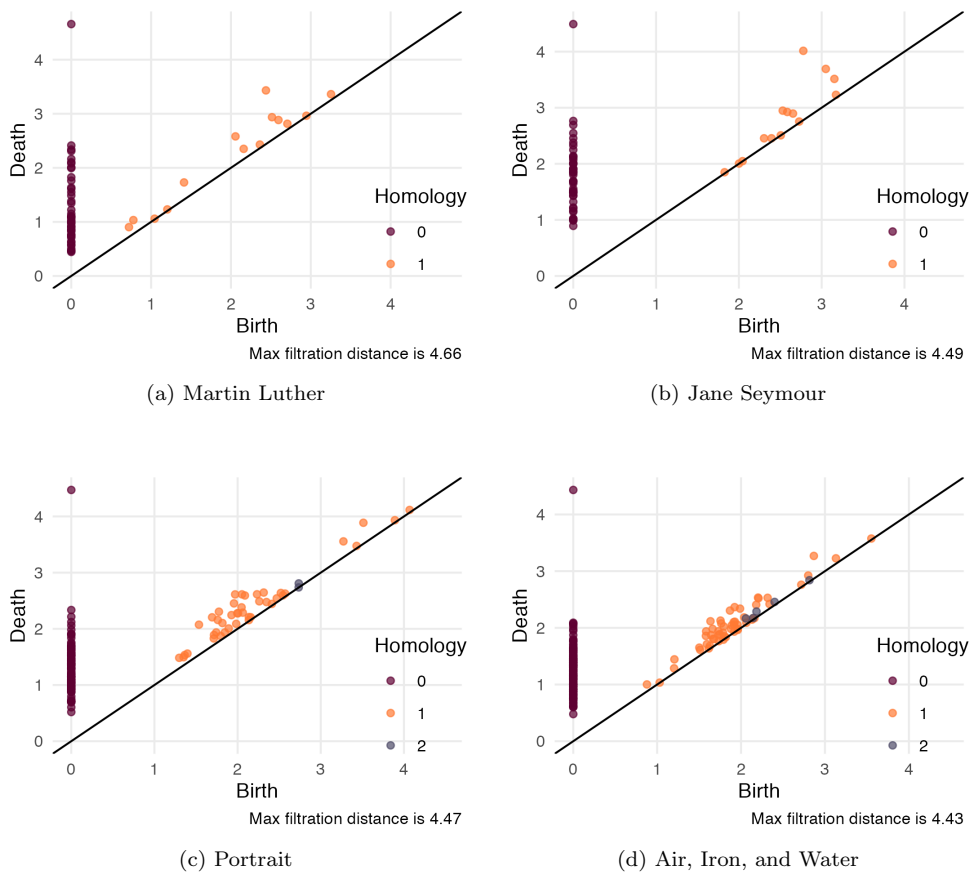


Figure 10: Persistence diagrams for Renaissance portraits in the top row and Cubist paintings in the bottom row. Displays birth of topological features up to dimension 3 on the x axis and death on the y and the maximum filtration distance

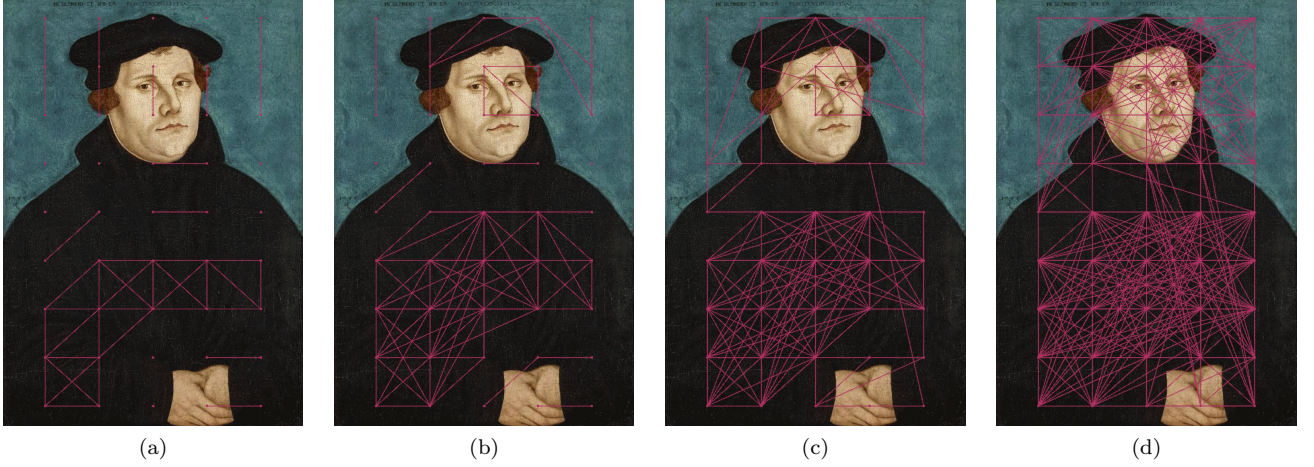


Figure 11: Skeleton plots of Vietoris-Rips simplicial complexes for Martin Luther at four fixed distance threshold values, where the axes are the x, y patch center coordinates

complex, with different textured and colored blocks from the orange-yellow in the top right to the dark purple-black in the bottom left. Although we can pick out the woman and her dress visually, there is more in common between the foreground and background here than in the hyper-realism of Renaissance portraiture with their uniform backgrounds.

Comparing filtrations over all artworks by movement, there is some evidence for different homology patterns. Figure 12 gets at this by overlaying the birth and death features over all painting-level filtrations. We can see that for H_0 , the deaths of Cubism components occur slightly later than that of Renaissance. The H_1 cycles also appear more persistent on average than that of Renaissance, as shown by the larger vertical radius of the green ellipse in panel 1. However at the extremes, shown in the lightest transparency indicate a larger left tail for Renaissance than for Cubism. That is, births and deaths of cycles (H_1) begin earlier in Renaissance works than in Cubist and Cubist works end slightly later. Also in the extremes, average persistence of any of the homologies 1, 2, and 0 are comparable.

In the second homology, holes, we can see that Cubism's births and deaths begin earlier, clustered between 1.5 and 2.5 on the x-axis while Renaissance is more dense between 2.5 and 3.5. But there are fewer points in this homology than in H_1 so this a noisier result.

Finally, there are only 3 observations in H_3 from Cubism paintings *Dinamica del Viento* and *Four Girls*.

Overall, the distributions are similar across all homologies but notably there are more Cubism outliers than Renaissance, as depicted in Figure 13. Notably this figure shows that particularly persistent H_1 cycles appear in the Renaissance portraits Martin Luther and Jane Seymour, but otherwise persistent cycles occur in *The Open Window*, *Four Girls*, and *Egg Beater*. As for H_2 holes, again *Four girls* and *The Open Window* appears as well as two Renaissance pieces: *Der Unglaubliche* and *Adoration of the Trinity*. *Dinamica del Viento* and *Four Girls* have the only two H_3 features that appear.

Interestingly *Dinamica del Viento* seems to be the most distinct painting of the bunch as it a textured chevron pattern with no obvious figures and leans towards Abstract art than Cubism. Perhaps

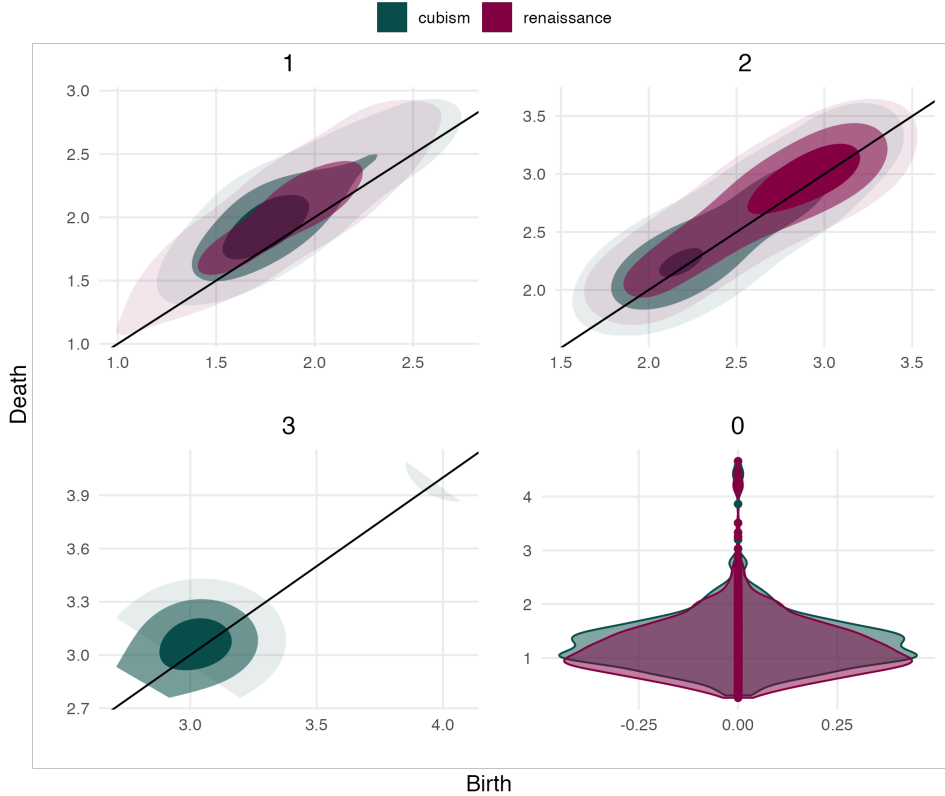


Figure 12: 2D density plots of Cubism and Renaissance individual artwork persistence diagrams for homologies 0-3

inclusion of Abstract works would share this H_3 homology, but for now I cannot draw conclusions about the meaning of this higher dimensional homology without more data.

5.2 Movement-level

One potential disadvantage of the filtration overlay plots above is the filtrations are computed separately, and we cannot discern connections between paintings and thus between movements. To this end, I construct a second dataset at the painting level in which each observation is a single patch from each painting, resulting in 20 observations and compute a filtration over this data. The centermost patches are selected from each artwork depicted in Figure 14.

From here, locational information is removed and the distance metric is constructed as the sum of the scaled textural and color features. Focusing again on H_0 components, I aim to look at which images are grouped together first within a network. Here, I run PCA again on the 20 observation dataset to extract a basis from which to project the vectors. From this we can already see clustering by movement with Renaissance works closer the right side of the figure and the Cubism pieces to the left.

In Figure 15 we see that Renaissance is more well connected than Cubism, something hinted at in the painting-level analysis in the overlapping densities of Figure 9. As we can see, Cubist paintings were some of the more persistent singletons with 8 (Portrait) and 9 (The Mud Bath) needing larger

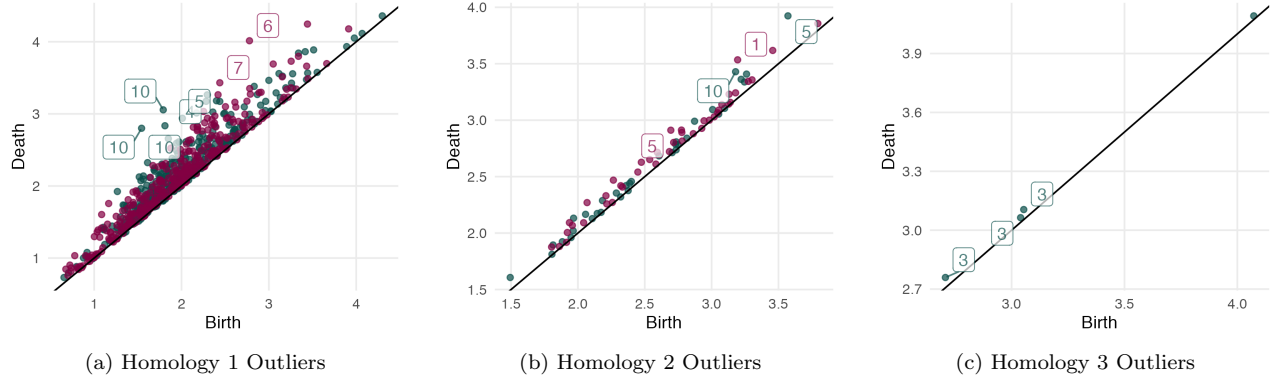


Figure 13: Persistence diagrams of Cubism and Renaissance individual artwork for homologies 1-3, large persistence components labeled with their painting and artist

distance thresholds to connect to the rest of the glob. The Mud Bath remains a singleton and is the final connected component, which makes intuitive sense as its color palette with its sharp, high value, high saturation red, yellow and blue is unlike any other painting. It lacks soft gradations from one hue to the next and leans more into its geometric composition than its figurative elements, though contains both. Art historian Millington describes The Mud Bath as influenced by Futurism and Vorticism, two avant-garde more abstract movements. Additionally, The Mud Bath was created during Bomberg’s early career of “vigorous vibrant abstraction” before he later incorporated more “expressive figuration” into his works [7].

Though I expected to see clustering into two connected components—with Cubism one and Renaissance the other, that is not what we see. In fact, the first edges are drawn between similar Cubist and Renaissance paintings: 10 (The Open Window) and 14 (Children’s Games). Several Cubist paintings are more similar to other Renaissance paintings than other Cubism paintings. With more artwork within each movement, we might see 2 connected components form along movement lines. Yet on the other hand, evidence here indicates Cubism is highly idiosyncratic, varying texturally and color-wise between paintings much more than Renaissance artworks.

This movement-level analysis comes with the most caveats. First, the dataset is small, and perhaps with more paintings included in each movement would reveal different persistent features, particularly in higher dimensions. Because the dataset is small each simplicial complex we construct over the images is inherently subject to higher variance. Also, the data is highly dependent upon the choice of a patch, so while the centermost patch is likely to contain essential figures and a moderately good representation of the entire piece, this certainly is not true for all paintings. And with more diverse patches within the artwork, finding a suitable representative patch is challenging. But at the cost of computational efficiency, one could construct the movement dataset at the painting level. This would mean computing wavelet decomposition and color moments across the entire painting.

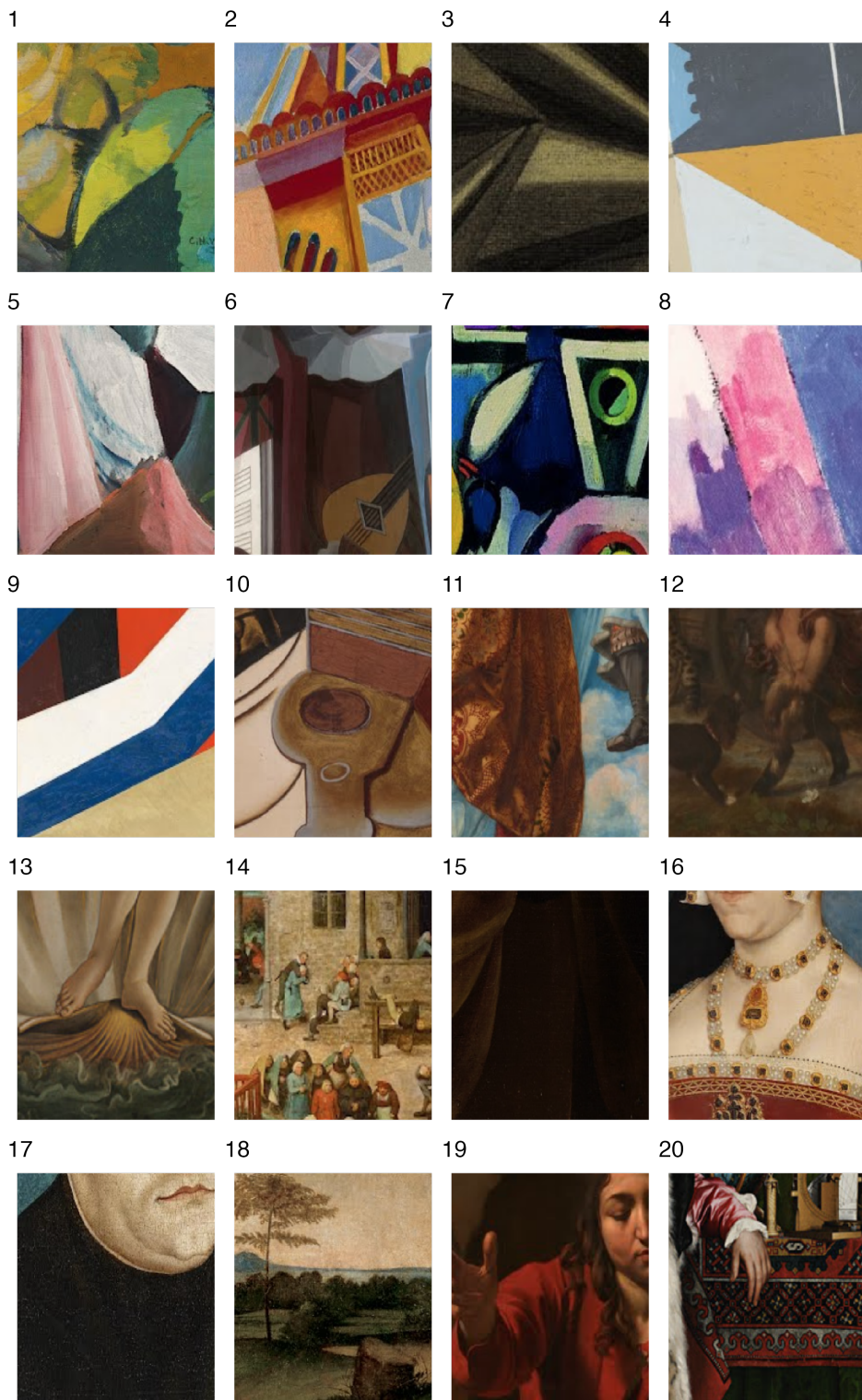


Figure 14: Patches used for movement-level analysis

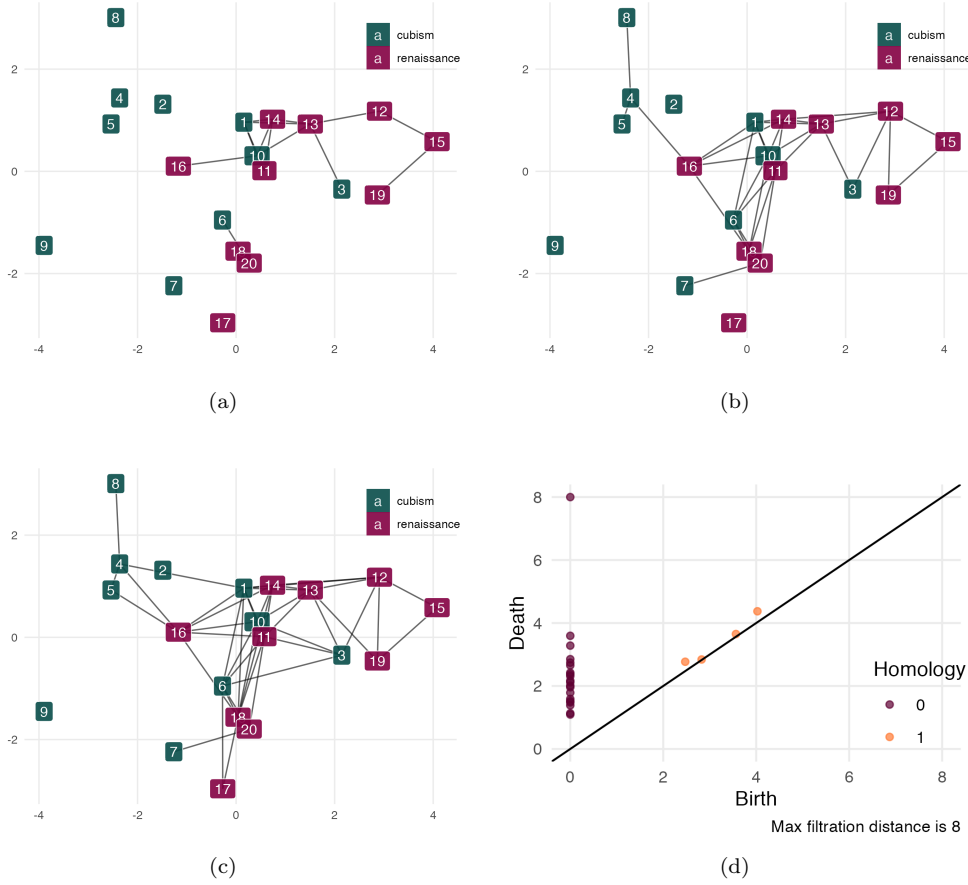


Figure 15: Panels (a)-(c) contain skeleton plots of Vietoris-Rips simplicial complexes for between-movement data at three fixed distance threshold values, where the axes are the x, y patch center coordinates, panel (d) contains persistence diagram over between-movement data

6 Conclusion

Based on the analysis of the patch-level dataset and the topological features extracted from the persistence charts of each artwork, Cubist paintings tend to exhibit more idiosyncratic features compared with Renaissance works. We see this in the movement-level analysis, that Cubist paintings do not cluster together as strongly into H_0 homologies as Renaissance works. Renaissance, on the other hand, gloms together into connected components based on similar features. Additionally, the painting-level persistence diagrams reveal Cubist artwork exhibits more complex and varied structures than Renaissance with its higher order homologies.

These findings suggest that Cubism is a more diverse and less cohesive art movement. This aligns with descriptions of Cubism as an experimental movement that sought to challenge traditional perspectives on art and break away from conventional modes of representation. In contrast, Renaissance art was characterized by a more unified aesthetic, with artists working within a shared set of visual conventions and techniques which imbued their works with a sense of realism. Artists of the time favored naturalistic representations of the human form and beauty, a reason for the greater topological cohesion revealed here.

While this study provides insight into combining wavelet analysis and color moments into topological features within artworks, there are many potential extensions in this area. One could adjust the distance metric in a number of ways, one of which weights texture more heavily than color. Because there are 6 color features and 3 texture features in this study, color weighs more heavily in the distance metric. This may overstate the idiosyncracy of Cubism since their color palettes share less overlap.

Additionally, future studies could expand the dataset to include more artworks both within the two movements and from a wider range of movements, allowing for a more comprehensive comparison of art history classifications. One could also leverage the wavelet coefficients themselves to assemble a dataset and filtrations upon these. By computing summary metrics based on wavelet coefficients (entropy, contrast, energy), some of the decomposition information is missed. A further analysis may also take a closer look at the higher dimensional homologies and incorporate these topological features into machine learning classification models that predict movement membership.

References

- [1] Hue, Value, Saturation | learn.
- [2] Renaissance art | Definition, Characteristics, Style, Examples, & Facts | Britannica, Mar. 2023.
- [3] GRAPS, A. An Introduction to Wavelets.
- [4] IJAZ, A. Wavelet analysis in R.
- [5] KRIEGER, L. Renaissance Painting Techniques, Mar. 2018.
- [6] LEE, B., SEO, M. K., KIM, D., SHIN, I.-S., SCHICH, M., JEONG, H., AND HAN, S. K. Dissecting landscape art history with information theory. *Proceedings of the National Academy of Sciences* 117, 43 (Oct. 2020), 26580–26590. Publisher: Proceedings of the National Academy of Sciences.
- [7] MILLINGTON, R. Art History | David Bomberg: mud baths & modernism, Jan. 2018.
- [8] REWALD, A. S. Cubism | Essay | The Metropolitan Museum of Art | Heilbrunn Timeline of Art History.
- [9] YANG, H., AND YANG, H. Evolution of Entropy in Art Painting Based on the Wavelet Transform. *Entropy* 23, 7 (July 2021), 883.

7 Code Description

To run the filtration, I use the ‘TDA’ package in R, specifically using the ‘ripsDiag’ function which computes a Vietoris-Rips filtration, with the settings for the maximum dimension to be 3, distance as Euclidean, and the maximum difference to be the mean distance, \bar{d} . This TDA package is an R wrapper/binding for the Dionysus C++ library which implements algorithms used to construct Vietoris-Rips complexes.

For an overview of the code, I run the following scripts in this order from the ‘source’ folder to produce everything in the ‘output’ folder:

```
create_image_features.R  
make_filtrations.R  
plot_image_features.R  
plot_pca.R  
plot_persistence.R  
animate_painting_filtrations.R  
animate_movement_filtration.R
```

The first script **create_image_features.R** reads in the set of images (in ‘input/images’, creates the grid of overlapping patches for each painting (via *construct_patch_centers(img, patch_size)* and *extract_patches(img, patch_centers)*), then over each patch computes *wavelet_decomposition()* (via the ‘waveThresh’ R package), extracts the coefficients (*extract_coefficients(decomp)*) from that wavelet decomposition, then computes the color moments (*compute_color_moments(patch)*), computes energy (*compute_energy(coefs)*), computes entropy (*compute_entropy(coefs)*), and finally computes contrast (*compute_contrast(coefs)*). These features are then saved in a row of a data frame with the function *create_patch_row(patch)* and this function is looped over all image patches. This script outputs the resulting patch level datasets over all paintings into the folder structure output/data/, with an example being output/data/cubism/egg-beater-2_stuart-davis.csv.

The second script **make_filtrations.R** reads in these source/data csv files and then computes distance matrices (*create_dist_matrix(data)*) across these source/data csv files. It then grabs the specified quantile in *make_filtration()* and puts that as the maximum distance threshold (for this paper I use quantile 50 but this can be adjusted if wanted). It then calls third party *ripsDiag()* function from the ‘TDA’ packages with the arguments specified as aforementioned. The birth and death of each feature is then saved as a data frame and exported to the folder set output/filtrations/ (with output/filtrations/egg-beater-2_stuart-davis/filt_df.csv being an example).

The third script **plot_image_features.R** plots the image textural and color features as ggplots and saves them in the output/plots folder. In this analysis I plot the features for individual paintings as they vary across the image patches in a painting with *plot_average_colorspace()* and *plot_feature()* (which maps over the texture and color features). The function *make_individual_plots()* reads in the underlying painting-level data for all paintings and wraps these two functions and exports the resulting plots. The

next function is *plot_movement_scatter()* which plots all combinations of features as a scatterplot and colors by movement. The function *plot_movement_hist()* plots the between movement distributions across all 9 features.

The fourth script **plot_pca.R** plots the PCA scatterplots shown in Figures 8 and 9. It relies on a function from ‘lib.R’, *run_pca()* which runs PCA over a data frame. The results are saved in ‘output/plots/pca’

The fifth script **plot_persistence.R** plots all 20 persistence diagrams via the output/data/cubism/|painting-name|/filt_df.csvs. It also plots the persistence density and scatterplot comparisons with *plot_persistence_compare(data, type = 'density', dimension)*. It also plots the labeled outlier plots of Figure 13 with *plot_persistence_paint_labels(data, dimen, quantile)*.

The final two scripts construct animations, some frames of which comprise Figures 11 and 15. This relies on the ‘simplicetree’ package which uses efficient data structures to store simplicial complexes. For individual paintings, I use *get_simplices(data)* which constructs a filtration over the data using *construct_simplex()* from **lib.R** (my implementation of a Vietoris-Rips filtration that was too slow to use throughout the paper, but can be used for smaller data). Once each step of the filtration with all simplicial complexes at each distance threshold defined, I iterate over all simplicial complexes in the filtration and plot just their edges with *plot_skeleton(nodes, coords, tree)* which is then called iteratively in *create_skeleton_animation(data, frames)* that produces a single image for each complex. These images are then compiled into a .gif file using the gifski(png_files) function and the still files are removed (unless otherwise specified). The **animate_movement_filtration.R** script works in much of the same way, but has a different plotting aesthetic as it plots the between movement filtration. At a later time, these two animation scripts will likely be consolidated into one.

Finally, **lib.R** is a library of helper functions accessed and used by multiple scripts.

This description of codebase is subject to change, with the latest version of the code and description available at <http://github.com/kobleary/art-explorer>.



(a) 1. Abstract Landscape,
Charles Walther (1919)



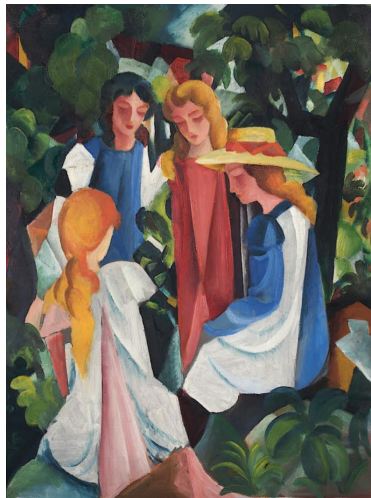
(b) 2. Air Iron and Water, Robert Delaunay (1937)



(c) 3. Dinamica del Viento, Emilio Pettoruti (1915)



(d) 4. Egg Beater No. 2, Stuart Davis (1928)



(e) 5. Four Girls, August Macke
(1914)

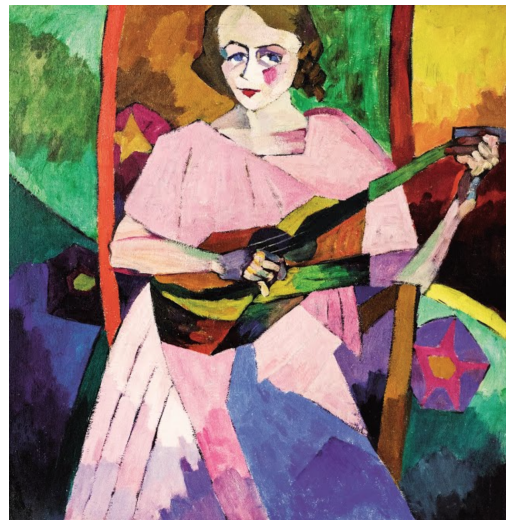


(f) 6. La Ultima Serenata, Emilio
Pettoruti (1937)

Figure 16: Cubist Images 1-6



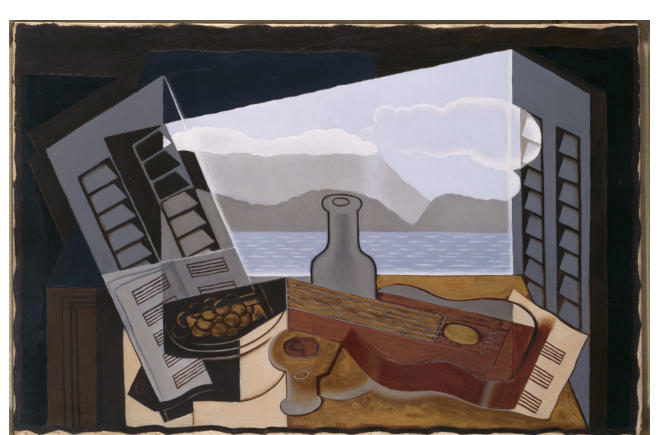
(a) 7. Popular Song and Bird from Brazil,
Amadeo Cardoso (1916)



(b) 8. Portrait, Aristarkh Lentulov (1913)



(c) 9. The Mud Bath, David Bomberg (1914)



(d) 10. The Open Window, Juan Gris (1921)

Figure 17: Cubist Images 7-10



(a) 11. Adoration of the Trinity Albrecht, Dürer (1511)



(b) 12. Bacchus and Ariadne, Titian (1520-1523)



(c) 13. Birth of Venus, Sandro Botticelli (1485-1486)



(d) 14. Children's Games, Pieter Bruegel the Elder (1560)



(e) 15. Der Unglaubliche, Thomas Caravaggio (1602)



(f) 16. Jane Seymour, Hans Holbein the Younger (1536)

Figure 18: Renaissance Images 1-6



(a) 17. Martin Luther, Lucas Cranach the Elder (1529)



(b) 18. Sleeping Venus, Giorgione (1510)



(c) 19. Supper at Emmaus, Caravaggio (1601)



(d) 20. The Ambassadors, Hans Holbein the Younger (1533)

Figure 19: Renaissance Images 7-10

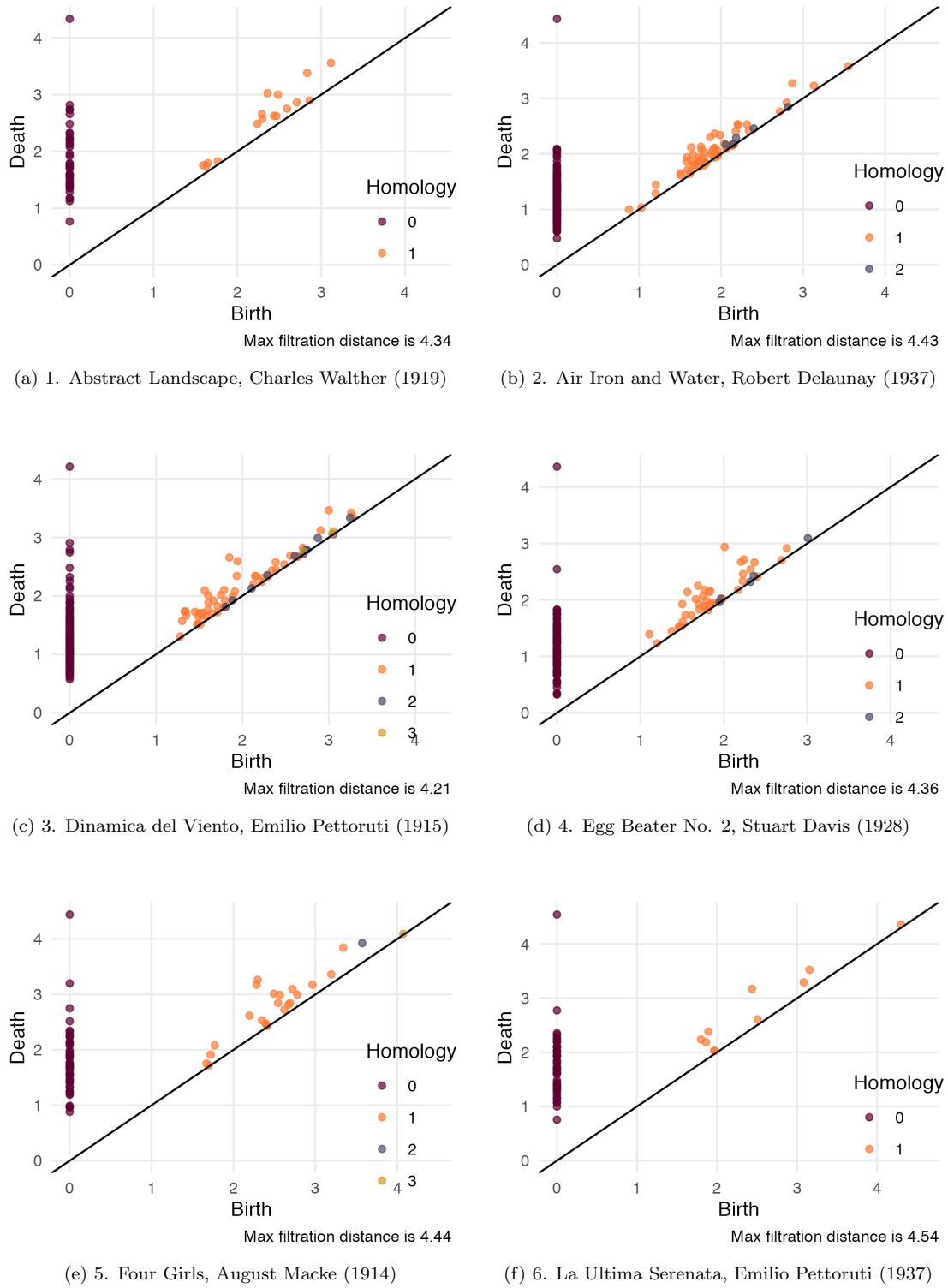
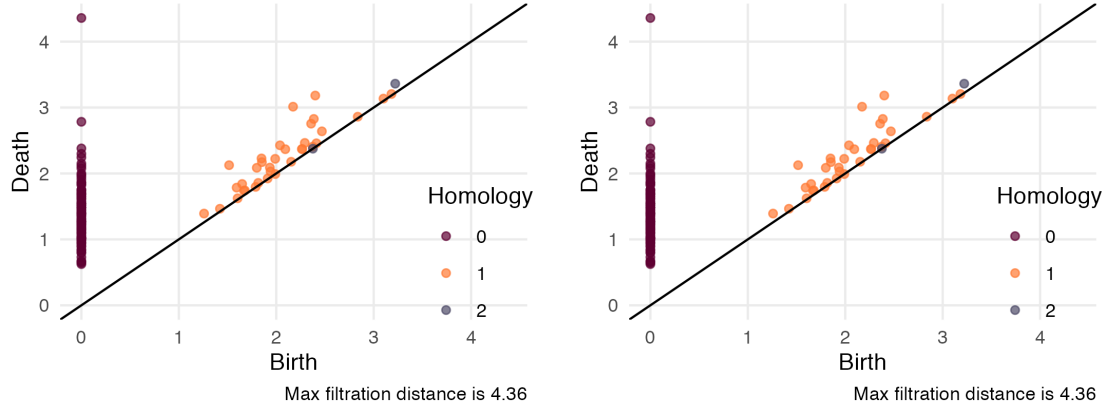
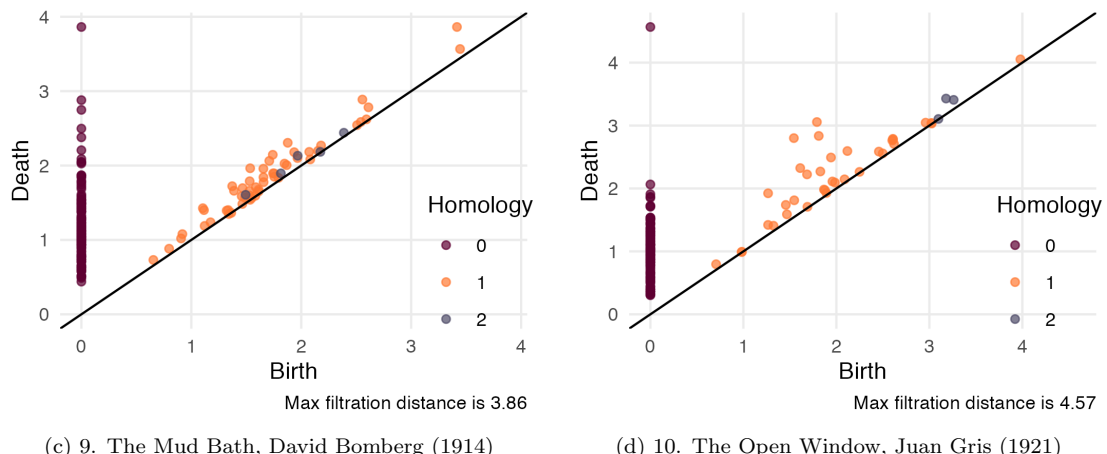


Figure 20: Cubism Filtrations 1-6



(a) 7. Popular Song and Bird from Brazil, Amadeo Cardoso (1916)

(b) 8. Portrait, Aristarkh Lentulov (1913)



(c) 9. The Mud Bath, David Bomberg (1914)

(d) 10. The Open Window, Juan Gris (1921)

Figure 21: Cubism Filtrations 7-10

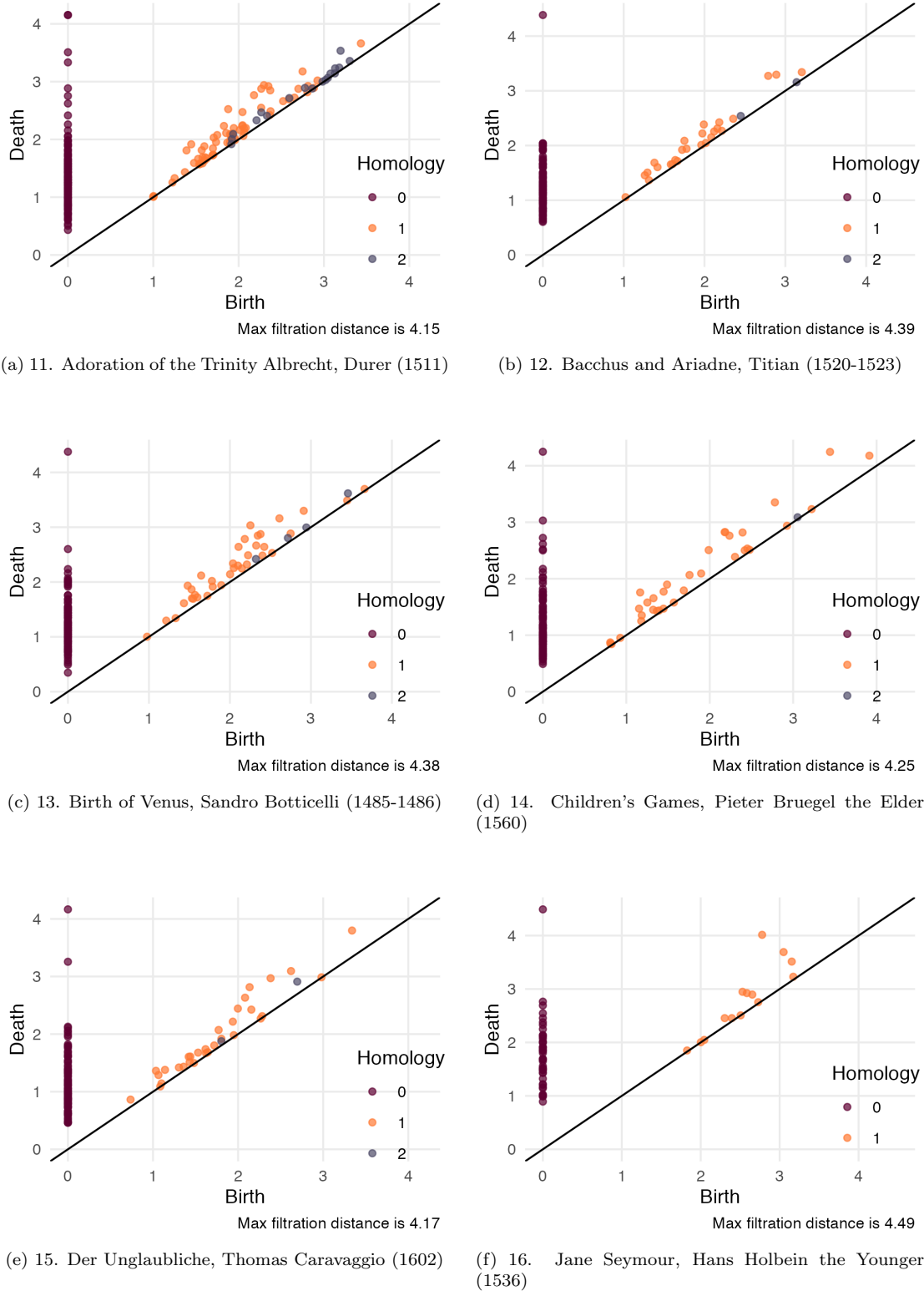


Figure 22: Renaissance Filtrations 11-16

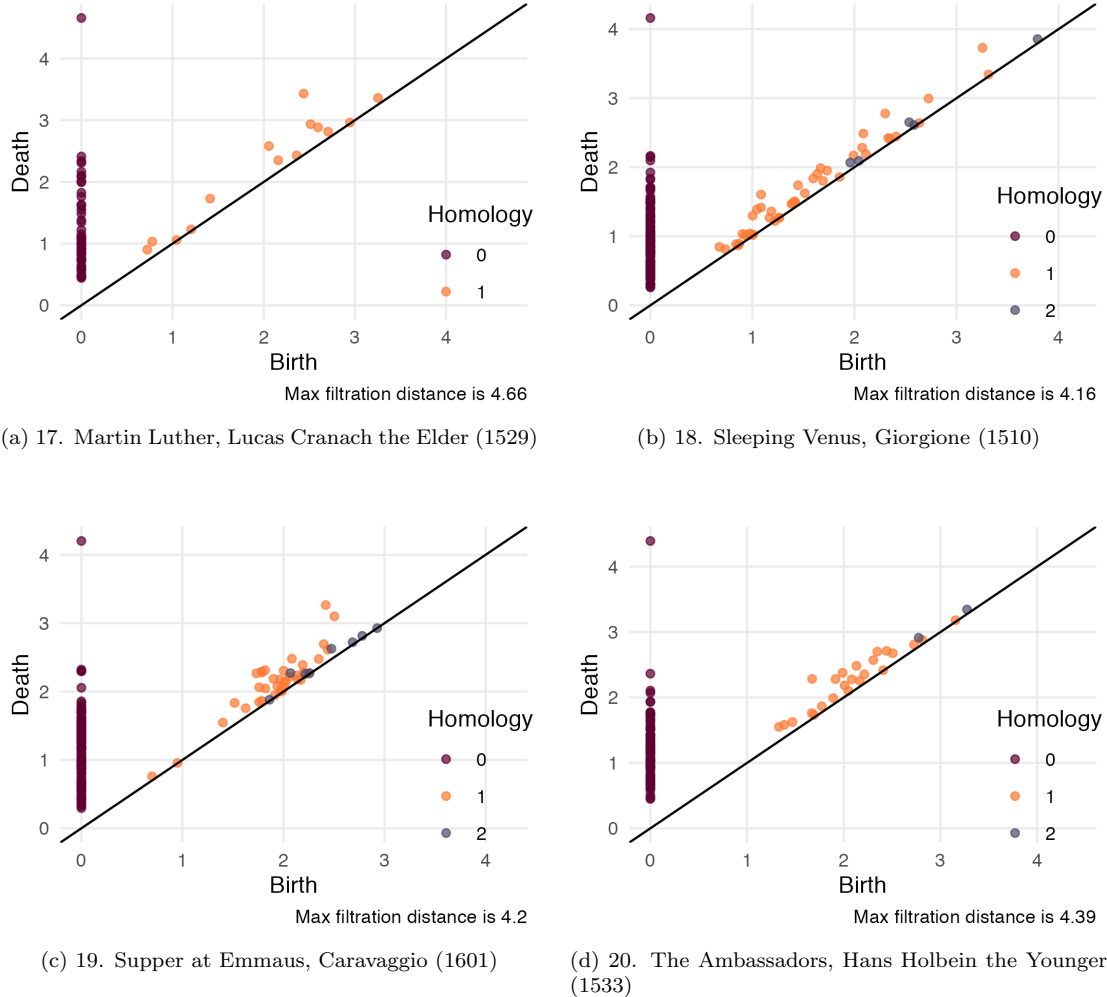


Figure 23: Renaissance Filtrations 17-20